Temperature Effect on Molecular Chirality：X-ray Diffraction and Neutron Diffraction Studies of D-alanine[*]

WANG, Wen-Qing   GONG, Yan   YAO, Nan

(*Department of Applied Chemistry, College of Chemistry and Molecular Engineering, Peking University, Beijing 100871*)

Abstract   The results of X-ray diffraction of single crystal D- and L-alanine at 300, 270, 250 K and neutron diffraction of D-alanine at 300, 260, 250, 240 K were presented to look for the static and dynamical structure feature of Salam phase transition. No change in the space group $P2_12_12_1$ symmetry was observed. The data rule out the hypothesis of a conventional structural phase transition and reveal a subtle and continuous symmetry breaking that occurs below ~250 K. A vibrationally generated electronic ring current model was explained the temperature effect on magnetic susceptibilities and opposite optical rotation phenomena related to the bond lengths of $\alpha C-H(2)$, $N(1)-H(1)$, $N(1)-H(4)$, and $N(1)-H(6)$ lengthening (or contraction). A picture of dynamic disorder due to the protonic motion was presented in the intermolecular hydrogen bonds between the NH_3^+ group and the CO_2^- group. Salam predicted the enhancement of parity-violating energy difference (PVED) due to temperature-induced phase transition. Tunneling dynamics of amino acids with PVED may provide a bifurcation mechanism for much faster development of homochirality.

Keywords：   Temperature effect, Phase transition,   X-ray diffraction,   Neutron diffraction,   D-alanine single crystal,   Parity-violating energy difference

In living systems, protein molecules are composed of twenty L-amino acids(only some amino acids of the opposite D-type do occur in cell walls of certain bacteria). The polynucleotides contain sugars in D-configurations only. Why is life based on L-amino acids and D-sugars rather than D-amino acids and L-sugars? The role of chirality in the theories that determine the origin of life remains a mystery and is a subject of intense debate[1-2]. Parity violation energy (E_{PV}) due to weak nuclear interaction between nucleons and electrons in chiral amino acid molecules provides a fundamental tool to understand the electronic behavior in living systems. Alanine is one of the amino acids encoded by codons with G(guanine) in the first position and went into proteins in very early life.

In 1991, Salam[3-5] proposed that chirality among the twenty amino acids of proteins may be a consequence of a phase transition (~250 K) under the influence of parity violation of electroweak force. We have performed seven kinds of experiments to verify the influence on the single crystal phase transition of D- and L-alanine and valine[6-12]. In 2003, Sullivan *et al*.[13] examined the temperature dependence of X-ray diffraction (296 and 258 K), ^{13}C solid-state NMR (298 to 249 K) and Raman spectra (298 to 271 K) for alanine and found no unusual behavior in their measuring temperature range. Two differential scanning calorimeters were used by Sullivan *et al*. to measure the transition behavior and heat capacities：a modulated differential scanning calorimeter (MDSC 2920) of TA instruments, Inc. and a DSC 820 from Mettler Toledo Inc. Both MDSC and DSC are of the heat-flux type. DSC measurements showed the heat transition at 270 K decreased with the number of recrystallizations suggesting a reduction in impurity level. They presented arguments against the Salam hypothesis and suspect our previous results[6].

On the other side, we used an adiabatic differential calorimeter with a continuous heating process at a pre-determined heating rate (0.5 ℃·min⁻¹). An obvious phase transition was shown from the discontinuity of specific heat at T_c both in the D-/ L-valine and D-/ L-alanine. To determine the ΔC between D-/L-form accurately, a twin sample (D-form on the sample holder, L-form on the reference holder) was employed. In order to maintain same temperature of the sample D-alanine (or D-valine) and the reference L-alanine (or L-valine), the system was operated with continuous heating power controlled by computer, independently. The differential specific heat was obtained by measuring

the heating rate (dT/dt=0.5 K·min^{-1} in the region of 77~300 K) of the valine ($m_{\text{D-Val}}=m_{\text{L-Val}}$=30.25 mg).

$$\Delta C=C_{\text{D-Val}}-C_{\text{L-Val}}=(P_1-P_2)/(m\,\text{d}T/\text{d}t)=P/(m\,\text{d}T/\text{d}t)$$

Here P is the power of auxiliary heater. The key of the experiment is to connect two high-sensitivity (10^{-9} V) voltmeters to the sample holder (D-valine) and reference holder (L-valine). The experimental results were repeated for the same samples after several thermal cycles (77 K⇔300 K). The sample chamber was pumped to high vacuum. The shape and magnitude of the specific heat jump and the peak position were almost the same for different cycles excluding any possibility of residual water or atmospheric moisture[14].

Besides, Barthes et al.[15] reported that the lattice dynamics of crystalline L-alanine showed unusual features with X-ray diffraction, which suggested the existence of a second order phase transition at 243~246 K. The MDSC 2920 of TA instrument was used is Barthes' experiments. Because of the larger speed of heating (5 ℃·min^{-1}), the temperature accuracy was not very good. However, the curve suggested that some kind of structural instability occured around this temperature. It was verified by the observation of ultrasound attenuation at 247 K by Wang's group[9], but it was undetected in Sullivans' work[13].

1　Experiment

1.1　Sample preparation and characterization

The single crystals of D- and L-alanine (Sigma Chemical Cooperation) used in X-ray diffraction analysis were grown by slow evaporation (2 to 3 weeks) from sterilization aqueous solution at 277 K, washed with absolute alcohol, evacuated and kept in a desiccator. The processes produced well-formed crystal elongated along the c axis. The sample crystals were of dimensions 1.00 mm×1.00 mm×0.70 mm (D-Ala) and 0.30 mm×0.40 mm×0.50 mm (L-Ala), respectively. The samples were characterized by elemental analysis (C, H, or N) and X-ray diffraction. The rotation angle (ξ) of D- or L-alanine solution was measured on Polarimeter PE-241 MC with wavelength 589.6 nm. By using the formula of $[\alpha]_{\text{D}}^{20}=\xi/(L\times c)$ ($[\alpha]_{\text{D}}^{20}$, rotatory power at 20 ℃；L：the path length；c：concentration of solutions of D- or L-alanine), the corresponding α values of D- and L- alanine were shown to be the same. The enantiomeric purity of D-, L- and DL-alanine (or valine) single crystal was identified by Chirasil-val capillary column of gas chromatography. Atomic force microscopy was used to characterize the surface of D- and L-alanine (or valine) crystals to detect the defects or micro bubbles[16-17].

The second batch of D- and L-alanine crystals used in neutron diffraction experiment [18] was prepared and characterized by Johnson's group in Oxford University. The single crystals were grown by slow evaporation from a methanol/water solution at

277 K, and were of dimensions 4 mm×2 mm×2 mm (L-Ala) and 7 mm×4 mm×1.5 mm (D-Ala).

1.2　Temperature-dependent X-ray diffraction of D- and L-alanine

The structure of L-alanine has been determined with X-ray crystallography by Simpson et al.[19] at room temperature and Destro et al.[20] at 23 K. Sullivan et al.[13] measured the X-ray diffraction data for D- and L-alanine crystals and reported that the unit cell dimensions at 296 and 258 K stayed the same. Barthes et al.[15] presented X-ray diffraction data of L-alanine and discovered an anomalous decrease of the lattice parameter c in discrete steps when heating the crystal from 10 K to room temperature. The present study is to look for the temperature dependence of crystal lattice torsion, the behavior of αC−H, the conformational change of NH$_3^+$ group, and the dihedral angle as a function of ΔE_{PV} of D- and L-alanine for proposed phase transition.

The unit cell dimensions and cell parameters of X-ray data were collected on a Rikagu RAXIS-RAPID imaging plate diffractometer with graphite monochromated Mo-K_{α} radiation (λ=0.071069 nm) at 300, 270 and 250 K (Table 1, Fig. 1). For example, the data were collected at a temperature of (250 ± 1) K to a maximum 2θ value of 54.9°. A total of 44 images, corresponding to 220.0° oscillation angles, were collected with 2 different goniometer settings. Exposure time was 1.00 min per degree. Indexing was performed from 1 oscillation which was exposed for 2.5 min. The camera radius was 127.40 mm. Readout was performed in the 0.100 mm pixel mode. Data were processed by the PROCESS-AUTO program package. Of the 3935 reflections collected, 600 were unique (R_{int}=0.026); equivalent reflections were merged. The linear absorption coefficient (μ) for Mo K_{α} radiation is 1.2 cm^{-1}. A symmetry-related absorption correction using the program ABSCOR was applied, which resulted in transmission factors ranging from 0.77 to 0.92. The data were corrected for Lorentz and polarization effects. A correction for secondary extinction was applied (coefficient is 1.64408×10^{-4}).

The structure was solved by direct methods(SAPI91) and expanded using Fourier techniques. The non-hydrogen atoms were refined anisotropically. Hydrogen atoms were refined isotropically. The final cycle of full-matrix-least-squares refinement was based on 600 observed reflections ($I > -10.00\ \sigma(I)$, I：measured intensities, $\sigma(I)$：estimated standard deviation) and 85 variable parameters and converged with unweighted and weighted agreement factors of (F_{o}：observed value, F_{c}：calculated value)：

$$R=\sum(F_{\text{o}}-F_{\text{c}})/\sum F_{\text{o}}=0.070$$

$$R_w=\sqrt{\sum w(F_{\text{o}}^2-F_{\text{c}}^2)^2/\sum w(F_{\text{o}}^2)^2}=0.078$$

$$R_1=\sum\|F_{\text{o}}|-|F_{\text{c}}\|/\sum|F_{\text{o}}|=0.030 \text{ for } I>2.0\ \sigma(I) \text{ data}$$

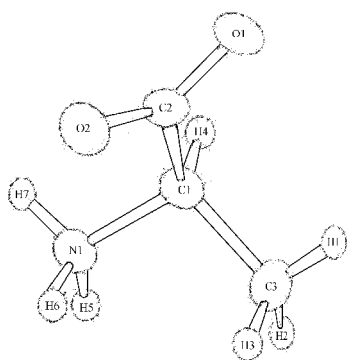The standard deviation of an observation of unit weight was

Fig.1 Crystal structure of D-alanine determined by X-ray diffraction

1.34. The weighting scheme was based on counting statistics and included a factor ($p=0.050$) to down weight the intense reflections. All calculation was performed using the teXsan crystallographic software package of Molecular Structure Corporation.

The crystal structure of L-alanine has been determined and refined by analysis of complete three-dimensional diffraction data from Mo X-radiation (Table 1). In the alanine crystal, the molecule is zwitterionic (^+H_3N–$C_2H_4COO^-$) and the nitrogen atom is coupled to three networks of intermolecular hydrogen bonds of unequal strength. The reduction in volume of L-alanine crystal with decreasing temperature is associated with a decrease of the lattice parameter (*a* and *b*), while *c* shows a small increase. These phenomena are coincided with Simpson[19] and Destro′s[20] data but undetected in Sullivan measurement[13], while the volume reduction and the lattice parameters (*b* and *c*) are concave-down at 270 K in D-alanine (Table 2).

Comparison with the X-ray data between different laboratories, we summarize that：First, the D- and L- alanines are orthorhombic and biaxial crystals. Because of the crystalline anisotropy, the assignment of the crystal axes (*a, b* and *c*) is important. The X-ray diffraction data of L-alanine from Simpson and Destro defined $a=0.6032$, $b=1.2343$, $c=0.5784$ nm (at 298 K). On the other side, Sullivan *et al.* defined $a=0.57811$, $b=0.60282$, $c=1.23401$ nm . Sullivan applied the magnetic field parallel to their longest axis (*c* axis), however, it is *b* axis in our case. Therefore, their findings on DC magnetic susceptibility do

Table 1 Temperature-dependent X-ray diffraction data of D- and L-alanine

Temperature	300 K		270 K		250 K	
Sample	D-Ala	L-Ala	D-Ala	L-Ala	D-Ala	L-Ala
Empirical formula	$C_3H_7NO_2$		Formula weight		89.09	
Mo-K_α	0.071069 nm		Crystal system		Orthorhombic	
Space group	$P2_12_12_1$		Z		4	
Unit cell	$a=0.60388(5)$	0.60344(5)	0.60073(5)	0.60095(5)	0.60041(3)	0.60002(4)
Dimensions	$b=1.23670(8)$	1.23668(8)	1.23030(7)	1.23388(7)	1.23179(5)	1.23293(6)
(nm)	$c=0.58000(2)$	0.57879(3)	0.57732(4)	0.57904(3)	0.57892(3)	0.57822(2)
Volume (nm^3)	0.43315(2)	0.43193(5)	0.42669(5)	0.42936(5)	0.42815(3)	0.42775(4)
D_{calc} / g·cm^{-3}	1.366	1.370	1.387	1.378	1.382	1.383
	$\alpha=90°$		$\beta=90°$		$\gamma=90°$	
Crystal dimensions	1.00 mm×1.00 mm×0.70 mm(D-Ala)			0.30 mm×0.40 mm×0.50 mm(L-Ala)		
$2\theta_{max}$	55.0°	54.8°	54.9°	54.9°	54.9°	54.9°
No. of reflections	3262	4077	3867	4092	3935	4076
Structure solution	Direct methods (MITHRIL 84)		Refinement		Full-matrix least-squares	
Function minimized	$\Sigma w(F_o^2-F_c^2)^2$	Least squares weights	$w=1/\sigma^2 (F_o^2)$		p-factor	0.05
Anomalous dispersion			All non-hydrogen atoms			
No. of observations	603	604	598	604	600	601
No. of variables	85	85	85	85	85	85
Reflection /Paramter ratio	7.09	7.11	7.04	7.11	7.06	7.07
Residuals: R; R_w	0.037; 0.047	0.086; 0.082	0.063; 0.078	0.060;	0.070; 0.078	0.056; 0.075
Residuals：R_1	0.036	0.032	0.029	0.0288	0.030	0.027
No. of reflections to calc R_1	596	596	592	596	593	589
Goodness of fit indicator	1.49	1.39	1.33	1.33	1.34	1.30
Max shift/error			0.000			
Max peak in final diff. map ×10^{-3} nm^3	0.26	0.25	0.25	0.22	0.27	0.19
Min peak in final diff. map ×10^{-3}nm^3	−0.17	−0.17	−0.15	−0.14	−0.16	−0.15

Table 2 Comparison with X-ray Diffraction data of L-/D-alanine by different laboratories

	Simpson[19]	Destro[20]	Sullivan[13]		This work					
	298 K	23 K	296 K	258 K	300 K		270 K		250 K	
	L-Ala	L-Ala	L-Ala	D-Ala	L-Ala	D-Ala	L-Ala	D-Ala	L	D-Al
a/nm	0.6032	0.5928(1)	0.57905(3)	0.57811(3)	0.60344(5)	0.60388(5)	0.60095(5)	0.60073(5)	0.60002(4)	0.60041(3)
b/nm	1.2343	1.2260(2)	0.60220(3)	0.60282(3)	1.23668(8)	1.23670(8)	1.23388(7)	1.23030(7)	1.23293(6)	1.23179(5)
c/nm	0.5784	0.5794(1)	1.23435(7)	1.23401(6)	0.57879(3)	0.58000(2)	0.57904(3)	0.57732(4)	0.57822(2)	0.57892(3)
V/nm^3	0.43064	0.42109	0.43005(4)	0.43005(4)	0.43193(5)	0.43315(2)	0.42936(5)	0.42669(5)	0.42775(4)	0.42815(8)

not concur with our report[6,10]. Second, Sullivan *et al.* varied the temperature from 296 K to 258 K but the unit cell dimensions stayed the same. These findings do not concur with other scientists[15,19-20] (Table 2).

From the X-ray data of Table 3, the important result is the apparent difference in the dihedral angle between D- and L-alanine at 250 K. The obvious dihedral angle change of D-alanine crystal (44.80°↔45.52°↔43.98°) must be caused by an alternation in the relative atomic position, however the αC−H bond length has no obvious variation in X-ray diffraction (Table 4).

2 Temperature-dependent neutron diffraction of D- alanine

According to our understanding, Salam phase transition is a dynamic structural phase transition. The high temperature phase is an ordered structure that becomes distorted below the transition temperature. In order to observe the geometric and dynamic structural changes involving the hydrogen atoms,

neutron data of D-alanine at 240, 250, 260, and 300 K are measured from VIVALDI (Very Intense Vertical Axis Laue Diffractometer) in EMBL-Grenoble Outstation by Dean Myles (Fig.2, Table 5). Unfortunately, L-alanine crystal was cracked in the middle process of the neutron diffraction, so we lack the L-alanine data for comparison.

2.1 Temperature-dependent dihedral angle (θ) of D-alanine

The calculation of the dihedral angle is based on the O(1) O(2)C(1)C(2)αH position (αH(4) in X-ray and αH(2) in neutron diffraction). The dihedral angle data of neutron diffraction concur with X-ray diffraction. In our experiments all the dihedral angles of D-alanine were 43°~ 45° in the crystalline state from 300→270→260→250→240 K, where ΔE_{PV} is negative values (namely, L-alanine is more stable than D-alanine). The observed trends indicated that parity-violation eff ects stabilize the zwitterions enantiomeric form of L-alanine, corresponding values of the dihedral angle close to 43°~ 45° (Table 6) and $\Delta E_{PV} \approx 0$[21-22].

**Table 3 X-ray data of dihedral angle of D- and L-alanine**

Temperature	300 K			270 K			250 K		
				D-alanine					
Atomic coordinates	X	Y	Z	X	Y	Z	X	Y	Z
O(1)	0.7281(2)	0.08438(7)	0.3716(1)	0.7280(1)	0.08419(6)	0.3723(1)	0.7282(1)	0.08412(6)	0.3727(1)
O(2)	0.4505(2)	0.18519(8)	0.2390(1)	0.4488(1)	0.18497(6)	0.2388(1)	0.4481(1)	0.18482(6)	0.2388(1)
αC(1)	0.4764(2)	0.1611(1)	0.6444(2)	0.4744(2)	0.16118(8)	0.6442(2)	0.4734(2)	0.16125(8)	0.6443(2)
C(2)	0.5604(2)	0.14163(8)	0.3975(2)	0.5591(2)	0.14146(7)	0.3978(1)	0.5582(2)	0.14134(7)	0.3980(1)
αH(4)	0.441(2)	0.238(1)	0.656(3)	0.441(2)	0.237(1)	0.656(2)	0.437(2)	0.237(1)	0.653(2)
Dihedral angle θ	44.80°			45.52°			43.98°		
				L-alanine					
	X	Y	Z	X	Y	Z	X	Y	Z
O(1)	0.7282(1)	0.08437(6)	0.3716(1)	0.7279(1)	0.08414(6)	0.3725(1)	0.7279(1)	0.08404(6)	0.3730(1)
O(2)	0.4503(1)	0.18512(7)	0.2388(1)	0.4480(1)	0.18484(6)	0.2387(1)	0.4480(1)	0.18484(6)	0.2387(1)
αC(1)	0.4766(2)	0.16118(8)	0.6444(2)	0.4736(2)	0.16115(7)	0.6445(2)	0.4736(2)	0.16115(8)	0.6447(2)
C(2)	0.5606(2)	0.14163(7)	0.3978(2)	0.5593(2)	0.14146(7)	0.3980(2)	0.5587(2)	0.14139(7)	0.3984(1)
αH(4)	0.440(2)	0.237(1)	0.655(3)	0.440(2)	0.238(1)	0.656(2)	0.440(2)	0.237(1)	0.658(2)
Dihedral angle θ	44.21°			45.20°			45.72°		

*The dihedral angle was calculated using the software of materials studio version 2.0, Accelrys Inc.

Table 4 X-ray data of bond lengths (×0.1 nm) of D- and L-alanine

	250 K		270 K		300 K	
	D-Ala	L-Ala	D-Ala	L-Ala	D-Ala	L-Ala
O(2)−C(2)	1.254(1)	1.257(1)	1.252(1)	1.256(1)	1.256(2)	1.257(2)
O(1)−C(2)	1.249(1)	1.246(1)	1.244(1)	1.244(1)	1.248(2)	1.244(2)
αC(1)−C(2)	1.534(1)	1.533(1)	1.530(1)	1.535(1)	1.539(2)	1.534(2)
αC(1)−C(3)	1.523(2)	1.523(2)	1.520(2)	1.523(2)	1.524(2)	1.524(2)
αC(1)−N(1)	1.491(2)	1.488(2)	1.488(2)	1.489(2)	1.497(2)	1.489(2)
αC(1)−αH(4)	0.95(1)	0.96(1)	0.96(1)	0.97(1)	0.97(2)	0.97(2)
N(1)−H(5)	0.98(2)	0.96(2)	0.96(2)	0.97(2)	0.97(2)	0.95(2)
N(1)−H(6)	0.91(2)	0.91(2)	0.92(2)	0.91(2)	0.92(2)	0.92(2)
N(1)−H(7)	0.89(2)	0.93(2)	0.92(2)	0.93(2)	0.93(2)	0.91(2)
C(3)−H(1)	0.97(2)	0.98(2)	0.99(2)	0.99(2)	1.03(2)	0.99(2)
C(3)−H(2)	1.00(2)	1.01(2)	0.99(2)	1.00(2)	0.98(2)	1.01(2)
C(3)−H(3)	0.99(2)	0.96(2)	0.99(2)	0.97(2)	0.97(2)	0.97(2)
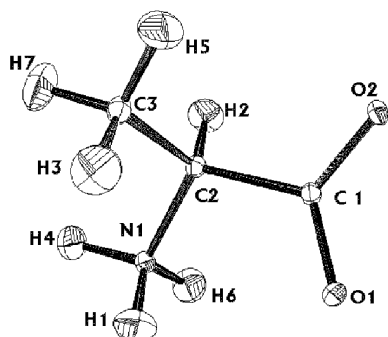
Fig.2 Neutron crystal Structure of L-alanine

These are states of definite parity not handedness, which is the "paradox" raised by Hund[23].

2.2 Temperature-dependent of torsion angle φ and ω of zwitterionic D-alanine

The spin-orbit coupling SCF wavefunction (SOC-SCF) was used to calculate the parity-violating energy of zwitterionic L-alanine by Kitayama *et al.*[24]. The $\Delta E_{PV}(=E_{PV,L}-E_{PV,D})$ map was created as a function of two torsion angles, φ for the NH_3 group and ω for the CO_2 group. The effect of the CH_3 group on the

Table 5 Temperature-dependent neutron diffraction data of D-alanine

T/K	a/nm	b/nm	c/nm	α	β	γ	V / nm^3
240	0.6008	1.2315	0.5792	90°	90°	90°	0.4285(10)
250	0.6009	1.2315	0.5791	90°	90°	90°	0.4285(9)
260	0.6015	1.2324	0.5793	90°	90°	90°	0.4294(9)
300	0.6007	1.2321	0.5793	90°	90°	90°	0.4288(1)

electronic structure is expected to be small. The ΔE_{PV} value varies from -4.8×10^{-20} to $+7.1\times10^{-20}$ hartree (1 hartree=27.2 eV= 4.36×10^{-18} J) in the (φ, ω) conformational space map, and the positive ΔE_{PV} area is wider than the negative one. In the present study, we found that the ω (CO_2 group) reduced from 18.613° (300 K) to 18.451°(240 K) and φ (NH_3 group) decreased from 60.217°(300 K) to 58.309°(250 K) then increased to 59.003° (240 K) in zwitterionic D-alanine (Table 7)

2.3 Bond lengths variation of N−H and αC−H in D-alanine

The existence of αC−H···O hydrogen bond in alanine has been proposed[25]. The bond length of αC−H increasing from 300 K to 250 K reflects the strength of intermolecular hydrogen

Table 6 Neutron data of dihedral angles (θ) of D-alanine

|	300 K			260 K			250 K			240 K		
	X	Y	Z	X	Y	Z	X	Y	Z	X	Y	Z
O(1)	−0.27059	−0.08405	−0.37155	−0.27138	−0.08401	−0.37332	−0.27215	−0.08407	−0.37296	−0.27187	−0.08447	−0.37320
O(2)	−0.54921	−0.18581	−0.23897	−0.55130	−0.18455	−0.23839	−0.55229	−0.18443	−0.23877	−0.55224	−0.18436	−0.23870
C(1)	−0.43969	−0.14129	−0.39839	−0.44101	−0.14107	−0.39837	−0.44137	−0.14113	−0.39852	−0.44185	−0.14123	−0.39835
αC(2)	−0.52262	−0.16121	−0.64614	−0.52577	−0.16136	−0.64501	−0.52577	−0.16140	−0.64497	−0.52621	−0.16110	−0.64497
αH(2)	−0.56544	−0.24720	−0.66372	−0.56633	−0.24748	−0.66331	−0.56710	−0.24778	−0.66223	−0.56890	−0.24673	−0.66050
θ		43.40°			45.08°			44.93°			44.31°	

*The dihedral angle was calculated using the software of materials studio version 2.0, Accelrys Inc.

Table 7 Neutron data of torsion angles of φ (NH$_3$ group) and ω (CO$_2$ group) of D-alanine

	300 K	260 K	250 K	240 K
ω(N–C–C–O)	18.613°	18.479°	18.484°	18.451°
$\Delta\omega$		0.134° ↓	0.005° ↑	0.033° ↑
φ(H–N–C–C)	60.217°	58.315°	58.309°	59.003°
$\Delta\varphi$		1.902° ↓	0.006° ↓	0.694° ↑

bonding (Table 8), which represents a significant contribution in the determination of molecular conformation of D-alanine and supports a magnetic phase transition of D-alanine at $T_c \approx 250$ K[10].

In the case of alanine crystal, the αC–H stretch generates an oscillating electronic current in a molecular ring, adjacent to the methine bond, which is closed to by hydrogen bonding (Fig.3) This oscillating ring current gives rise to a magnetic dipole transition moment (m). The bond lengths of N(1)–H (1), N(1)–H(4) and N(1)–H(6) display different behavior. When the temperature reduced from 300 to 250 K, the αC–H lengthening in D-alanine, negative current flowing in the direction N→αC when electrons are injected into the ring, produces a magnetic dipole transition moment with a component in the direction of the electric dipole transition moment(μ). The rotation strength, $R=$ Im($\mu \cdot m$), is negative as observed experimentally. The main difference between enantiomers lies in the fact that they produce opposite optical rotation due to the opposite sign of Im ($\mu \cdot m$). From the Freedman model[26], we can make a sound explanation of the observed low temperature magnetic susceptibility behavior of D- and L-alanine crystals[10]. To account for these unusual effects, it is presented a picture of dynamic disorder due to the proton transport in the intermolecular hydrogen bonds. The
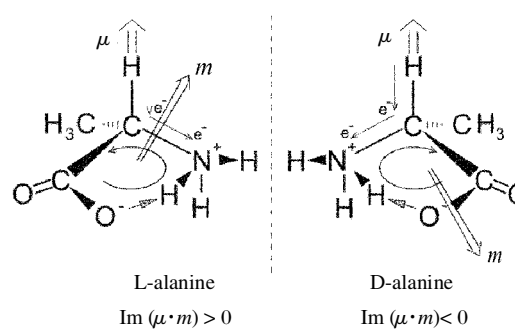
Fig.3 Vibrationally generated ring currents in alanine enantiomer

breaking of the N–H···O(1) accompanied with the orientation of the NH$_3^+$ group and formation of the new N–H···O(2) hydrogen bond with neighboring molecule in the unit cell[27].

3 Conclusion and remarks

1) X-ray scattering techniques were utilized to study the static properties of the correlation functions and the temperature dependence of the order parameter. Neutron scattering techniques were unrivaled in studying of the dynamics of structural phase transitions. Specific heat and magnetic susceptibility reflect the long-wavelength response, which provides averaged properties of the fluctuations. Neutron scattering provides a direct measurement of the two-particle correlation function for all wave vectors and frequencies. The dynamic behavior of the –CH$_3$, –NH$_3^+$ and –CO$_2^-$ group produces complex spin relaxation mechanisms accompanied with spectral diffusion processes in the crystalline lattice[27].

2) No change of the space group symmetry was observed. The data rule out the configuration transition from D- to L-

Table 8 Neutron data of bond lengths(×0.1 nm) of D-alanine

	240 K		250 K		260 K		300 K	
C(1)–O(1)	1.247(3)	1.246(3)*	1.245(2)	1.245(2)*	1.246(3)	1.248(3)*	1.244(4)	1.246(5)*
C(1)–O(2)	1.257(3)	1.256(3)	1.259(3)	1.259(3)	1.259(3)	1.259(3)	1.255(4)	1.260(5)
C$_\alpha$(2)–C(1)	1.535(4)	1.535(4)	1.535(3)	1.535(3)	1.537(4)	1.537(4)	1.536(4)	1.539(5)
C$_\alpha$(2)–N(1)	1.489(3)	1.489(3)	1.485(2)	1.485(2)	1.489(3)	1.490(3)	1.484(3)	1.479(4)
C$_\alpha$(2)–C(3)	1.527(3)	1.527(3)	1.524(2)	1.524(2)	1.522(3)	1.524(3)	1.515(3)	1.516(5)
N(1)–H(1)	1.031(4)	1.031(4)	1.035(4)	1.034(4)	1.027(5)	1.027(5)	1.028(6)	1.039(8)
N(1)–H(4)	1.052(5)	1.056(5)	1.052(4)	1.052(4)	1.043(5)	1.043(5)	1.054(6)	1.051(9)
N(1)–H(6)	1.040(5)	1.041(5)	1.042(4)	1.042(4)	1.032(5)	1.033(5)	1.028(6)	1.040(9)
C$_\alpha$(2)–H$_\alpha$(2)	1.092(4)	1.089(4)	1.097(4)	1.097(4)	1.094(4)	1.094(4)	1.091(5)	1.095(8)
C(3)–H(3)	1.080(6)	1.080(6)	1.080(6)	1.080(6)	1.081(7)	1.081(7)	1.074(8)	1.070(12)
C(3)–H(5)	1.092(6)	1.093(6)	1.095(6)	1.095(6)	1.080(7)	1.081(7)	1.085(8)	1.077(12)
C(3)–H(7)	1.091(7)	1.088(7)	1.111(7)	1.110(7)	1.102(8)	1.102(8)	1.082(9)	1.100(15)

*The values for the heavy-heavy bond lengths were corrected for thermal motion effects (using the TLS method)

transformation but reveal a subtle and continuous symmetry breaking that occurs below 250 K. Salam hypothesis predicted a second order phase transition, which amplifies the electroweak force and parity-violating energy difference. An asymmetric double-well potential model with a tiny PVED in the depths of the two potential wells, can lead to the enrichment of L-alanine[28-30].

Recently, Rakvin *et al.*[30] carried out heat capacity (C_p) and electron spin echo measurements on L-alanine at cryogenic temperature. The obtained C_p data show the "Boson peak" (as seen a maximum in C_p/T^3 versus T plots) in the low temperature region (1.8~20 K). They provided a mechanism for the spin-lattice relaxation process at cryogenic temperature. The first transition was related to the $\alpha H(2)$ proton on the neighboring L-alanine molecule and the second was related to the H(4) proton on the NH_3^+ group. Since their study was at very low temperature, most of the intramolecular motions were frozen out and the residual dynamics should be related mainly to intermolecular motions. They concluded that the boson peaks are intrinsic properties of the alanine lattice. It was shown that, in a crystal with a hydrogen-bonded network, these modes could display orientational disorder character. What could be the origin of the disorder in L-alanine? The question of the origin of the homochirality of life is still far from being answered. The temperature-dependent heat capacity C_p of D-alanie single crystal with Quantum Design PPMS is required to test the "Boson peak" further.

Acknowledgments

References

1   Hegstrom, R. A.; Kondepudi, D. K. *Sci. Am.,* **1992**：98

2   Avetisov, V.; Goldanski, V. *Proc. Natl. Acad. Sci. USA,* **1996, 93**：11435

3   Salam, A. *Phys. Lett. B,* **1992, 288**：153

4   Salam, A. *J. Mol. Evol.,* **1991, 33**：105

5   Salam, A. Chemical evolution：Origin of life. Hampton Virginia, USA：Deepak Publishing, 1993：101

6   Wang, W. Q.; Yi, F.; Ni, Y. M.; Zhao, Z. X.; Jin, X. L.; Tang, Y. Q. *J. Biol. Phys.,* **2000, 26**：51

7   Wang, W. Q.; Liang, Z. *Acta Phys.-Chim. Sin.,* **2001, 17**(12)：1077 [王文清, 梁 智. 物理化学学报(*Wuli Huaxue Xuebao*), **2001, 17**(12)：1077]

8   Wang, W. Q.; Gong, Y.; Li, C. *Chinese Science Bulletin,* **2002, 47**(7)：603 [王文清, 龚 炎, 李 晨. 科学通报(*Kexue Tongbao*), **2002, 47**(7)：603]

9   Wang, W. Q.; Min, W.; Zhu, C. F.; Yi, F. *Phys. Chem. Chem. Phys.,* **2003, 5**：4000

10   Wang, W. Q.; Min, W.; Bai, F.; Sun, L.; Yi, F.; Wang, Z. M.; Yan, C. H.; Ni, Y. M.; Zhao, Z. X. *Tetrahedron：Asymmetry,* **2002, 13**：2427

11   Wang, W. Q.; Min, W.; Liang, Z.; Wang, L. Y.; Chen, L.; Deng, F. *Biophys. Chem.,* **2003, 103**：289;
Wang, W. Q.; Min, W.; Liang, Z.; Wang, L. Y.; Chen, L.; Deng, F. *Biophys. Chem.,* **2003, 106**：96

12   Chen, Y.; Wang, W. Q.; Du, W. M. *Acta Phys. -Chim. Sin.,* **2004, 20**(5): 540 [陈 渝, 王文清, 杜为民. 物理化学学报(*Wuli Huaxue Xuebao*), **2004, 20**(5): 540]

13   Sullivan, R.; Pyda, M.; Pak, J.; Wunderlich, B.; Thompson, J. R.; Pagni, R.; Pan, H.; Barnes, C.; Schwerdtfeger, P.; Compton, R. *J. Phys. Chem. A,* **2003, 107:** 6674

14   Yang, H. S.; Lou, F. M.; Wang, W. Q.; Sheng, X . R.; Zhuang, Z. Z.; Shi, L.; Chen, Z. J. *Chin. Phys. Lett.,* **1995, 12**(5): 297

15   Barthes, M.; Bordallo, H. N.; Dénoyer, F.; Lorenzo, J.-E.; Zaccaro, J.; Robert, A.; Zontone, F. *The European Physical Journal B,* **2004, 37:** 375

16   Wang, W. Q.; Gong, Y.; Liang, Z.; Sun, F. L.; Shi, D. X.; Gao, H. J.; Lin, X.; Jiang, P.; Wang, Z. M. *Surf. Sci.,* **2002, 512:** L379

17   Guo, H. M.; Liu, H. W.; Wang, Y. L.; Gao, H. J.; Gong, Y.; Jiang, H. Y.; Wang, W. Q. *Surf. Sci.,* **2004, 552:** 70

18   Wang, W. Q.; Liu, Y. N.; Gong, Y. *Acta Phys.-Chim. Sin.,* **2004, 20**(11): 1345 [王文清, 刘轶男, 龚 奕. 物理化学学报(*Wuli Huaxue Xuebao*), **2004, 20**(11): 1345

19   Simpson, H. J.; Marsh, R. E. *Acta Cryst.,* **1966, 20:** 550

20   Destro, R.; Marsh, R. E. *J. Phys. Chem.,* **1988, 92:** 966

21   Berger, R.; Quack, M. *Chem. Phys. Chem.,* **2000, 1:** 57

22   Kikuchi, O.; Wang, H. *Bull. Chem. Soc. Jpn.,* **1990, 63:** 2751

23   Hund, F. *Z. Physik.,* **1927, 43:** 805

24   Kitayama, T.; Kiyonaga, H.; Morihishi, K.; Talahashi, O.; Kikuchi,

O. *J. Mol. Struc.-Theochem.,* **2002, 589-590:** 183

25 Vargas, R.; Garza, J.; Dixon, D. A.; Hay, P. B. *J. Am. Chem. Soc.,* **2000, 122:** 4750

26 Freeman, T. B.; Balukjian, G. A.; Nafie, L. A. *J. Am. Chem. Soc.,* **1985, 107:** 6213

27 Barthes, M.; Vik, A. F.; Spire, A.; Bordallo, H. N.; Eckert, J.

J. Phys. Chem. A, **2002, 106：** 5230

28 Loh, E. *J. Chem. Phys.,* **1975, 63**(8): 3192

29 Lee, K.; Shin, S.; Ka, J. *J. Mol. Struc. (Theochem),* **2004, 679:** 59

30 Rakvin, B.; Maltar-Stmecki, N.; Ramsey, C. M.; Dalal, N. S. *J. Chem. Phys.,* **2004, 120**(14): 6665

分子手性的温度效应：D-丙氨酸的变温 X 衍射和中子衍射研究 [*]

王文清　　　龚龑　　　姚楠

（北京大学化学与分子工程学院，应用化学系，北京　100871）

摘要　利用 X 衍射（300, 270, 250 K）和中子衍射（300, 260, 250, 240 K）研究 D-丙氨酸单晶在静态的和动力学的变温过程中的结构特征以及考证 Salam 预言的由 D 到 L 构型转变的可能性. 实验发现丙氨酸晶体的空间群 $P2_1 2_1 2_1$ 对称性没有改变. 实验结果否定了构型相变的可能，但是发现在~250 K 有一个微小的、连续的对称性破缺发生. 晶体分子振动产生的环电流模型可以用来解释 D- 和 L-丙氨酸单晶直流磁化率和天然旋光角相反的现象，与之相关的中子衍射数据进一步揭示了变温过程中 αC–H(2), N–H(1), N–H(4), N–H(6) 键长的不同变化. 中子衍射还显示了质子移动所导致的动力学无序，来源于分子内氨基和羧基形成的氢键和分子间 αC–H 和氨基形成的氢键，从而产生的晶格扭曲和 NH_3^+ 的扭转. 实验表明 Salam 预言相变不是传统意义的结构相变，而是由于温度效应导致了在相变点附近分子的宇称破缺能差（PVED）增大，然后通过氨基酸分子的隧道效应扩大了宇称破缺能差的影响，这一研究为生命现象中快速的均一手性形成提供了非线性机理的合理解释.

关键词：　温度效应，相变，X 衍射，中子衍射，D-丙氨酸单晶，宇称破缺能差
中图分类号：　O641